Journal of
Nanoscience and Nanotechnology
Vol. 11, 3284–3290, 2011

Synthesis of β-Cyclodextrin-Modified Water-Dispersible Ag-TiO_2 Core–Shell Nanoparticles and Their Photocatalytic Activity

Indrajit Shown, Masaki Ujihara, and Toyoko Imae*

Graduate Institute of Engineering, National Taiwan University of Science and Technology, 43 Keelung Road, Section 4, Taipei 106-07, Taiwan

The β-cyclodextrin-modified Ag-TiO_2 core–shell nanoparticles were prepared by sodium borohydrate reduction of $AgNO_3$ and the subsequent hydrolysis of the tetraisopropyl orthotitanate in an aqueous medium. Inversely in the preparation of β-cyclodextrin-modified TiO_2-Ag core–shell nanoparticles, first hydrolysis and then following reduction were carried out. The synthesized spherical core–shell nanoparticles were highly water-dispersible and had an average diameter in the range of 9 to 12 nm. A significant shifting of surface plasmon band was observed for the synthesized Ag-TiO_2 and TiO_2-Ag core–shell nanoparticles. On a model reaction, namely, the photodegradation of phenol by the UV light irradiation, the photocatalytic property of TiO_2 nanoparticles was enhanced, when the Ag nanoparticle was embedded in the core of TiO_2 nanoparticles but TiO_2 nanoparticles coated by Ag shell decreased the photocatalytic property of TiO_2 nanoparticles. The mechanism is ascribed to the surface plasmon characteristics of Ag in the core of the TiO_2 nanoparticles under the acceleration by host–guest inclusion characteristics.

Keywords: β-Cyclodextrin, Water-Dispersible Nanoparticle, Surface Plasmon, Photocatalysis, Photodegradation, Ag-TiO_2 Core–Shell, TiO_2-Ag Core–Shell.

RESEARCH ARTICLE

1. INTRODUCTION

Over the past years the metal and metal oxide nanoparticles have received significant attention due to their optical, electronic, catalytic and plasmonic properties.[1–4] Especially the core–shell nanostructures with improved catalytic efficiency have great importance in comparison with the simple monometallic nanoparticles.[5,6] In the metal–metal oxide nanoparticles, oxide shell protects the metallic core from the corrosive environment in a catalytic system.[7,8] A number of core–shell nanomaterials such as Au-SiO_2, Au-TiO_2, Au-ZrO_2, Ag-SiO_2, Ag-TiO_2, Ag-ZrO_2 and ZnS:Mn-SiO_2 with emerging properties and applications have been synthesized.[9,10]

Among such core–shell nanostructures the Ag-TiO_2 is quite attractive because of its several additional properties besides the individual ones of Ag and TiO_2 nanoparticles. The TiO_2 has attracted much attention in the field of photocatalysis and solar cell applications,[11,12] meanwhile the Ag is well known for the chemical and biological sensing applications.[13,14] It is also known that the combination of the Ag-TiO_2 as a core–shell nanomaterial in a favorable way dramatically enhances the photophysical and catalytic properties by indirectly influencing the interfacial charge transfer processes.[15] Additionally the thin shell of porous TiO_2 can help to diffuse the ions and molecules through it and to change the dielectric constant.[16,17] However the TiO_2 shell usually leads to aggregation of particles and decreases the active surface area. Thus the synthesis of mono-dispersive and stable core–shell nanoparticle is a challenging task.

There are several reports available on the various synthesis methods of Ag-TiO_2 core–shell nanoparticles.[18–21] Most of these synthesis methods for Ag-TiO_2 core–shell nanoparticles involved dimethylformamide and surfactants. Recently Vaidya et al.[22] synthesized the uniform Ag-TiO_2 core–shell nanoparticles using reverse micellar route. The organic solvents and surfactants are both toxic and are not easily degraded in the natural environment. Therefore it is needed to modify the surfaces of Ag-TiO_2 core–shell nanoparticles by biocompatible molecules so as to develop some eco-friendly materials by green pathway and mild conditions for biocompatible photocatalytic applications.

*Author to whom correspondence should be addressed.

 1533-4880/2011/11/3284/007 doi:10.1166/jnn.2011.3764

Cyclodextrins (CDs) are a truncated cone-shaped, non-toxic, cyclic oligosaccharide with a hollow apolar cavity. The supramolecular chemistry of CDs has been the subject of extensive investigations because of its well known ability on the formation of host–guest inclusion complex and on molecular recognition for various different types of molecules.[23] Surface absorption of β-cyclodextrin (β-CD) on a semiconductor particle has been found to improve the charge transfer rate from the photo-excited semiconductor to the guest molecule as an electron acceptor in the β-CD cavity.[24,25] The synthesis of the metal and metal oxide nanoparticles protected by CDs has been reported.[26–28] In particular CD-modified nanoparticles are highly dispersed in aqueous system and would improve catalytic activity.

Recently it has been found that β-CD acts as a very effective stabilizer on the preparation of colloidal core–shell metallic nanoparticles.[29] However, no one has reported the fabrication of β-CD-modified water-dispersible Ag-TiO_2 core–shell nanoparticles, as far as we know. In this article, water-dispersible normal and reverse Ag-TiO_2 core–shell nanoparticles are synthesized by using β-CD as a capping agent at moderate condition (room temperature). The optical properties, structure and composition of the metal–metal oxide core–shell particles were characterized by UV-visible absorption spectroscopy, transmission electron microscopy (TEM) and X-ray photoelectron spectroscopy (XPS). Finally the photocatalytic activity of the synthesized Ag-TiO_2 core–shell nanoparticles was also investigated in water and compared with the TiO_2 nanoparticles without Ag. Phenol was used for the determination of methodology on a reaction of the photocatalytic degradation. To the best of our knowledge, this is the first example on the photocatalytic application of water-dispersible Ag-TiO_2 core–shell nanoparticles, which are simple and environment-friendly system.

2. EXPERIMENTAL DETAILS

2.1. Reagents

Silver nitrate, tetraisopropyl orthotitanate and isopropanol were purchased from Wako chemicals. Phenol, 4-aminoantipyrine and potassium ferricyanide were purchased from Acros Organics. β-CD was purchased from Junsei Chemical Ltd. All reagents were of analytical grade and used without further purification. Ultrapure (Millipore Milli-Q) water was used for all synthesis and in the catalytic study.

2.2. Instruments

UV-visible absorption spectra for dispersions were collected with a Jasco V-670 spectrophotometer using a 10 mm quartz cell. The microscopic observation was performed on a Hitachi H-7000 TEM with a CCD camera attachment, operating at 100 kV. Samples for TEM were prepared by casting a droplet of the dispersion on a copper grid, which was coated with a thin carbon film. XPS analysis was performed on a theta probe ESCA VG Scientific (2002) using a monochromatic AlKα as the exciting source. The samples were prepared by spin-coating one drop of a nanoparticle dispersion on a Si-substrate and then allowing them to dry in air. Photoirradiation was carried out under atmosphere, using a HOYA EX250 UV light source with a 250-W Hg lamp (below 320 nm).

2.3. Synthesis of Monometallic Ag and TiO_2 Nanoparticles

Ag nanoparticles were synthesized as below. After 0.0792 g of β-CD was dissolved in 9.795 cm^3 of water under stirring, 0.1 cm^3 of NaOH (1 M) was added to the solution so as to adjust pH between 10 and 12. To this solution, 0.1 cm^3 of an aqueous $AgNO_3$ (10 mM) solution was added under stirring, and sequentially 0.005 cm^3 of a $NaBH_4$ (10 mM) solution was slowly added with continuous stirring at room temperature. The stirring was continued for 2 hr. The solution turned yellow immediately after adding $NaBH_4$, indicating the formation of particles in the solution.

TiO_2 nanoparticles were prepared by hydrolysis of $[(CH_3)_2CHO]_4Ti$ in an aqueous solution of β-CD. First 0.0792 g of β-CD was dissolved in 9.400 cm^3 of water and then a solution was adjusted pH between 10 and 12 by adding 0.1 cm^3 of NaOH (1 M) under continuous stirring. Moreover 0.5 cm^3 of isopropanol solution of $[(CH_3)_2CHO]_4Ti$ (10 mM) was slowly added under vigorous stirring at room temperature and the solution was continuously stirred for 2 hr. The resultant solution was almost transparent and very stable.

2.4. Synthesis of Ag-TiO_2 and TiO_2-Ag Core–Shell Nanoparticles

Ag-TiO_2 core–shell nanoparticles were synthesized by adding dropwise 0.5 cm^3 of an isopropanol solution of $[(CH_3)_2CHO]_4Ti$ (10 mM) to 10 cm^3 of a solution of preformed Ag nanoparticles with vigorous stirring. During the progress of the reaction, the yellow solution of Ag nanoparticles slowly converted to brownish yellow, indicating the formation of Ag-TiO_2 particles in the solution. The final concentrations of the Ag and TiO_2 in the metal–metal oxide particles were calculated to be 0.1 and 0.5 mM, respectively.

For the synthesis of TiO_2-Ag core–shell nanoparticles, 0.1 cm^3 of an $AgNO_3$ (10 mM) solution was added to 10 cm^3 of a solution of preformed TiO_2 nanoparticles with vigorous stirring. To the solution, 0.005 cm^3 of an aqueous solution of $NaBH_4$ (10 mM) was added with stirring at room temperature and the stirring was continued for 2 hr. The color-less solution slowly turned pale reddish purple after adding $NaBH_4$, indicating the formation of

RESEARCH ARTICLE

TiO_2-Ag particles in the solution. Here the final concentrations for TiO_2 and Ag were calculated to be 0.5 and 0.1 mM, respectively.

Using the same procedure, Ag-TiO_2 core–shell nanoparticles with different TiO_2 concentrations from 0.1 to 0.4 mM were synthesized at a constant Ag concentration (0.1 mM). For the synthesis of TiO_2-Ag core–shell nanoparticles, the Ag concentration was changed from 0.1 to 0.4 mM with the fixed concentration of TiO_2 (0.1 mM).

All the dispersions of nanoparticles were remained stable in ambient condition without changing their colors.

2.5. Photocatalytic Degradation

The photocatalytic activities of Ag-TiO_2 (0.1:0.5 mM) and TiO_2-Ag (0.5:0.1 mM) core–shell nanoparticles and TiO_2 (0.5 mM) nanoparticles were studied by measuring the photodegradation rates of phenol. For a typical photodegradation, 5 cm^3 of a stock solution of phenol (100 g/m^3) was mixed with 5 cm^3 of the solutions of nanoparticles and stirred for 1–2 min. The concentration of TiO_2 nanoparticles was definite at approximately 0.25 mM. For all examinations of photocatalytic degradation, the phenol concentration was maintained constant at 50 g/m^3. The aqueous solutions of phenol-containing nanoparticles were photoirradiated by using a UV light source under atmosphere at room temperature. The degradation of phenol was monitored by 4-aminoantipyrine according to an ultraviolet ratio method:[30] At every 5–10 min an aliquot was withdrawn from the reaction mixture. The phenol concentration was determined by measuring the UV-visible absorbance (at 510 nm) of the solutions in existence of 4-aminoantipyrine (3 wt%) and potassium ferricyanide (2 wt%) and by comparing with the calibration curve.

3. RESULTS AND DISCUSSION

3.1. Synthesis of β-CD-Modified Core–Shell Nanoparticles

Ag-TiO_2 core–shell nanoparticles were prepared by one pot synthesis that involved reduction of silver ions with $NaBH_4$ in the presence of β-CD and succeeding hydrolysis of the tetraisopropyl orthotitanate in water. The resultant solution was almost transparent and very stable. The silver ions were reduced first with $NaBH_4$, followed by the slow hydrolysis of tetraisopropyl orthotitanate to make a TiO_2 shell over the Ag core. Then the β-CD plays an important role as a protecting agent and stabilizer for nanoparticles. Inversely for the water-dispersible TiO_2-Ag core–shell nanoparticles, first the TiO_2 nanoparticles were synthesized and followed by the addition of $AgNO_3$ and $NaBH_4$, leading to the deposition of metal Ag on the TiO_2 nanoparticles. A schematic representation of the preparation of Ag-TiO_2 and TiO_2-Ag core–shell nanoparticles is shown in Scheme 1.

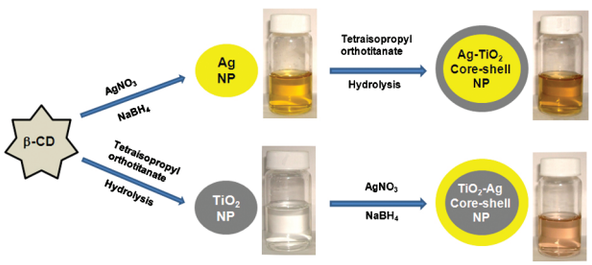

Scheme 1. Schematic representation of the preparation of β-CD-modified Ag-TiO_2 and TiO_2-Ag core–shell nanoparticles. NP: nanoparticle.

3.2. Photophysical Property of β-CD-Modified Core–Shell Nanoparticles

The surface plasmon property of the metal nanoparticles is a great importance in the study of the metallic nanomaterials. Then the coherent oscillation of the free electron is generated on the surface of metallic nanoparticles and the absorption of an external electron field occurs due to the resonance. Figure 1 shows the UV-visible absorption spectra of TiO_2 and Ag nanoparticles prepared at alkaline pH in the presence of β-CD as a stabilizer. Due to the plasmonic excitation resonance, the solution of Ag nanoparticles revealed a Plasmon band at 405.5 nm. The transparent solution of TiO_2 nanoparticles provided strong UV absorption below 330 nm but no absorption above 330 nm. The formation of the Ag-TiO_2 and the TiO_2-Ag core–shell nanoparticles was confirmed by a UV-visible

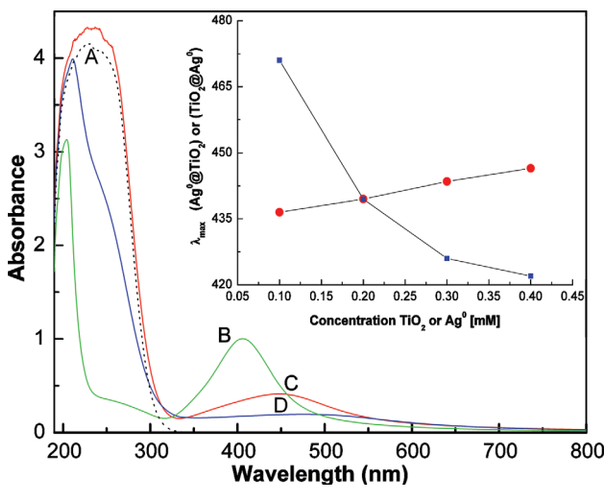

Fig. 1. UV-Vis absorption spectra of β-CD-modified nanoparticles in water. (A) TiO_2 (0.5 mM), (B) Ag (0.1 mM), (C) Ag-TiO_2 core–shell (0.1:0.5 mM), (D) TiO_2-Ag core–shell (0.5:0.1 mM). Inset: surface plasmon bands (λ_{max}) of β-CD-modified core–shell nanoparticles as a function of Ag or TiO_2 concentration from 0.1 to 0.4 mM. (•): Ag-TiO_2 (at a constant Ag concentration of 0.1 mM), (■): TiO_2-Ag (at a constant TiO_2 concentration of 0.1 mM).

absorption spectroscopy, as seen in Figure 1. The TiO_2-Ag and Ag-TiO_2 core–shell nanoparticles exhibited a surface plasmon band of Ag in the visible region. This band was strongly influenced by metal oxide (TiO_2), although TiO_2 itself has no absorption in the visible region above 330 nm. The surface plasmon bands of the Ag-TiO_2 and the TiO_2-Ag core–shell nanoparticles are significantly red-shifted to be at 447.5 and 448.0 nm respectively, in comparison with that (405.5 nm) of Ag nanoparticles. The high dielectric constant of the TiO_2 metal oxide causes a red-shift in the surface plasmon band of Ag.[7]

To clarify the photophysical properties of the TiO_2-Ag and Ag-TiO_2 core–shell nanoparticles, positions of the surface plasmon bands are plotted in Figure 1(inset) as a function of Ag^+ and Ti^{4+} concentrations, respectively. A plasmon band of the Ag-TiO_2 core–shell nanoparticles was red-shifted when the TiO_2 concentration was changed from 0.1 to 0.4 mM, keeping Ag concentration constant at 0.1 mM. This is attributed to the effect of thickness of TiO_2 shell on plasmon phenomenon of Ag nanoparticle. On the other hand, on the TiO_2-Ag core–shell nanoparticles (respect to TiO_2 concentration at 0.1 mM), a plasmon band from thin Ag shell (0.1 mM) was remarkably red-shifted from that (405.5 nm) of Ag nanoparticle by the strong effect of TiO_2 core. However, the affect weakened, that is, a plasmon band was blue-shifted, when the Ag concentration (or shell thickness) increased, indicating the approach of core–shell nanoparticle to homogeneous Ag nanoparticle or the diminution of the effect of TiO_2. When the core (TiO_2) concentration of TiO_2-Ag core–shell nanoparticles was high (0.5 mM) (Ag^+ concentration is 0.1 mM) (see Fig. 1), the effect of TiO_2 was less than that at core concentration of 0.1 mM. This should be due to the formation of too thin Ag layer or the nonuniform coverage by Ag metal on the surface of TiO_2 core.

3.3. Morphology and Size Distribution of β-CD-Modified Core–Shell Nanoparticles

TEM images of the β-CD-modified nanoparticles are shown in Figure 2(A–D). It can be seen that the nanoparticles were a sphere and fairly small, although the sizes are different each other. The average diameters of the Ag (0.1 mM) and TiO_2 (0.5 mM) nanoparticles were 6.4 ± 1.9

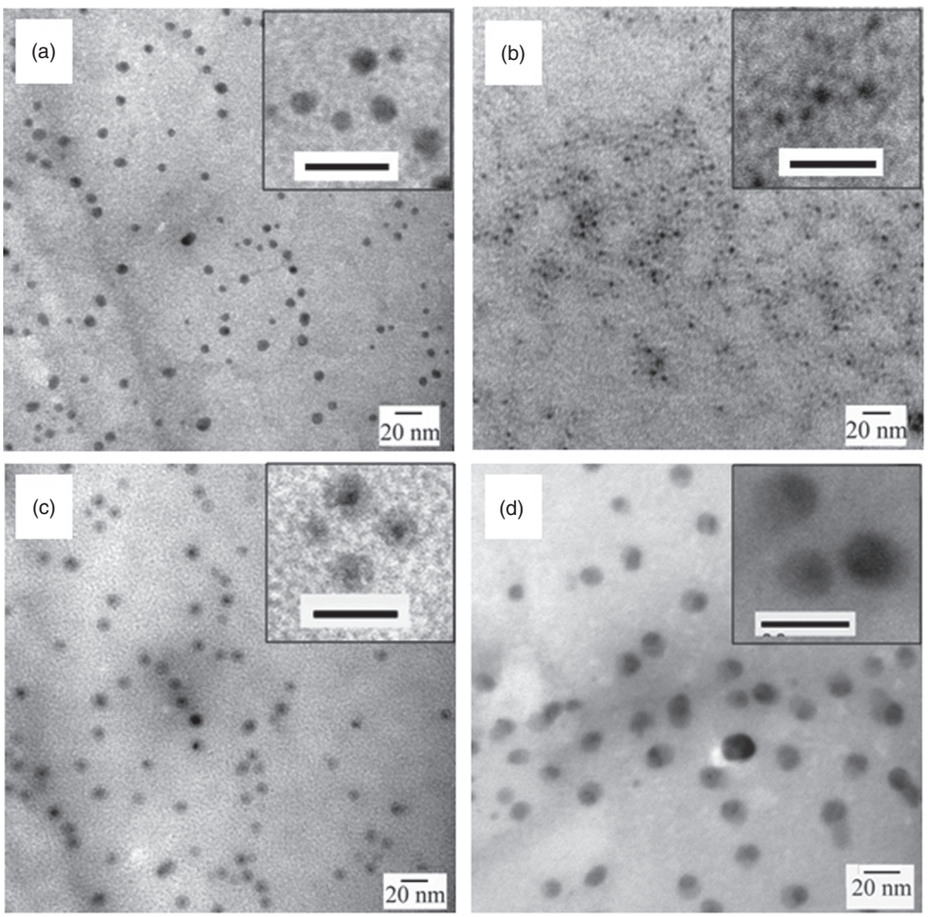

Fig. 2. TEM images of β-CD-modified nanoparticles. (a) Ag (0.1 mM), (b) TiO_2 (0.5 mM), (c)Ag-TiO_2 core–shell (0.1:0.5 mM), (d)TiO_2-Ag core–shell (0.5:0.1 mM). The scale bar in inset is 20 nm.

RESEARCH ARTICLE

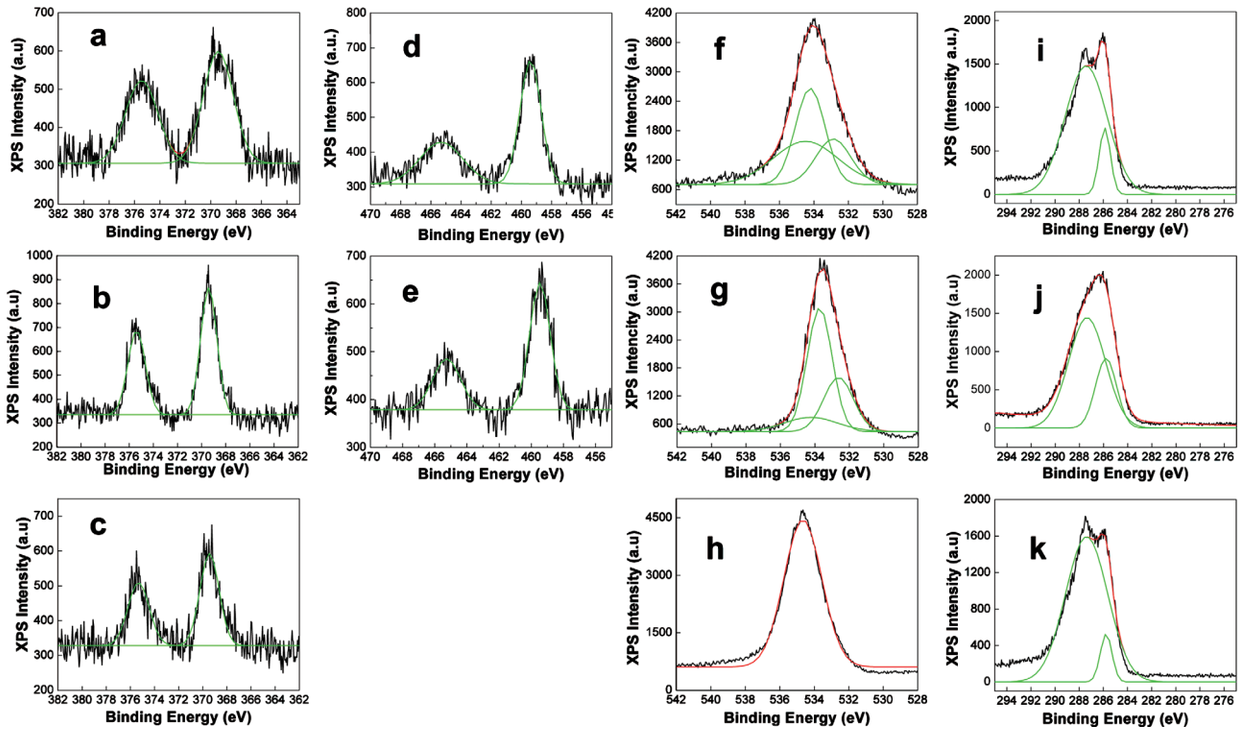

Fig. 3. X-ray photoelectron spectra of β-CD modified nanoparticles (a) Ag 3d (Ag-TiO_2 core–shell), (b) Ag 3d (TiO_2-Ag core–shell), (c) Ag 3d (Ag), (d) Ti 2p (Ag-TiO_2 core–shell), (e) Ti 2p (TiO_2-Ag core–shell), (f) O 1s (Ag-TiO_2 core–shell), (g) O 1s (TiO_2-Ag core–shell), (h) O1s Ag (i) C1s (Ag-TiO_2 core–shell), (j) C1s (TiO_2-Ag core–shell), (k) C1s Ag.

and 4.5 ± 1.0 nm, respectively, from histograms of size distribution of nanoparticles (300 samples). It was observed for the Ag-TiO_2 (0.1:0.5 mM) and TiO_2-Ag (0.5:0.1 mM) core–shell nanoparticles that their particle sizes were 9.1 ± 1.0 and 11.3 ± 1.0 nm respectively. These results mean that the particle size is almost uniform with a narrow size distribution. Additionally, in the Ag-TiO_2 core–shell nanoparticles the outer shell of the TiO_2 metal oxide was clearly observed round the core of Ag. The formation of the Ag shell was also observed for the TiO_2-Ag core–shell nanoparticles but the shell thickness was not uniform round all the TiO_2 surfaces. This result is consistent with the result described above. Thus the TEM images support the formation of the Ag-TiO_2 and TiO_2-Ag core–shell nanoparticles.

3.4. Composition of β-CD Modified Core–Shell Nanoparticles

In order to confirm the detail composition of the β-CD modified nanoparticles, XPS analysis was carried out. The XPS spectra of Ag-TiO_2 core–shell (0.1:0.5 mM), TiO_2-Ag core–shell (0.5:0.1 mM) and Ag (0.1 mM) nanoparticles are shown in Figure 3. Although each spectrum of Ag and Ti atoms displays two isolated peaks, that of O and C atoms consists of one asymmetric peak or two unisolated peaks. Therefore the O and C peaks were decomposed by using a Gaussian fitting program. Thus obtained binding energies of component peaks are listed in Table I. In the both core–shell nanoparticles as well as Ag nanoparticles the Ag $3d_{3/2}$ and Ag $3d_{5/2}$ peaks of the metallic silver were commonly observed at 369.4 and 375.4 eV, respectively. The peaks observed at 285.8 and 287.4 eV for three nanoparticles can be ascribed to C 1s which comes from the β-CD on the preparation process of nanoparticles.

Table I. Binding energy of β-CD-modified Ag-TiO_2 core–shell (0.1:0.5 mM), TiO_2-Ag core–shell (0.5:0.1 mM) and Ag (0.1 mM) nanoparticles.

	Binding energy (eV)		
Composition	Ag-TiO_2	TiO_2-Ag	Ag
C 1s	285.9	285.8	285.8
	287.4	287.4	287.4
O 1s	532.9	532.6	534.3
	534.2	533.7	
	534.5	534.2	
Ag 3d5/2	375.4	375.4	375.3
Ag 3d3/2	369.4	369.4	369.4
Ti 2p1/2	465.3	465.3	—
Ti 2p3/2	459.4	459.4	—

Both Ag-TiO_2 and TiO_2-Ag core–shell nanoparticles show two Ti $2p_{1/2}$ (465.3 eV) and Ti $2p_{3/2}$ (459.4 eV) peaks with the peak separation value of 5.9 eV. These binding energy values provide evidence of Ti^{4+} oxidation

RESEARCH ARTICLE

state. Meanwhile it should be noticed that three components of O atoms were observed for Ag-TiO_2 and TiO_2-Ag core–shell nanoparticles but only one component was for Ag nanoparticles. The minor two C 1s peaks at 532.7 ± 0.2 eV (surface bridging O_2 in TiO_2) and 534.3 ± 0.2 eV (adsorbed O_2) were common for Ag-TiO_2 and TiO_2-Ag core–shell nanoparticles. However a main O 1s peak at 534.1 ± 0.3 eV was observed for three nanoparticles due to the O atom of β-CD. All the observed binding energy values match well with the values in literature.[21,31] The binding energy data indicate that the Ag-TiO_2 and TiO_2-Ag core–shell nanoparticles are mainly composed of Ag, Ti, O and C, although in the Ag nanoparticles only Ag, O and C were found. Namely, the former consists of Ag, TiO_2 and β-CD, and the component of the latter is Ag and β-CD, as expected.

3.5. Photocatalytic Activity of β-CD Modified Core–Shell Nanoparticles

The plasmon band at visible region of the Ag-containing TiO_2 nanoparticles should support the enhancement of photocatalysis. The photocatalytic degradation property of the β-CD-modified Ag-TiO_2 (0.1:0.5 mM) core–shell nanoparticles was compared with those of the β-CD-modified TiO_2-Ag (0.5:0.1 mM) core–shell nanoparticles and β-CD-modified TiO_2 (0.5 mM) nanoparticles by carrying out irradiation of UV light on 50 g/m^3 phenol. According to the procedure described in the experimental section, the degradation of phenol (in %) was calculated and its variation was plotted in Figure 4 as a function of irradiation time. It is noticed that the degradation of phenol occurred in the order of Ag-TiO_2 core–shell nanoparticles > TiO_2 nanoparticles > TiO_2-Ag core–shell nanoparticles > no photocatalyst. This order also can be confirmed from the kinetic analysis.

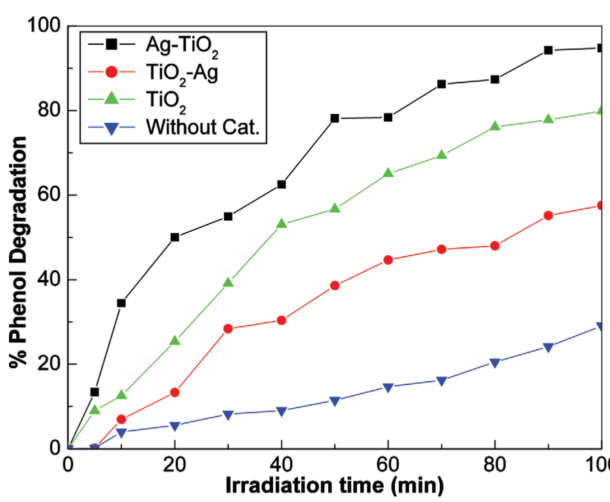

Fig. 4. Photocatalytic degradation of phenol under UV light irradiation [250 W Hg lamp (below 320 nm)] in atmosphere at room temperature in the presence of Ag-TiO_2 core–shell (■), TiO_2-Ag core–shell (•), and TiO_2 nanoparticles (▲) and in the absence of nanoparticles (▼).

The reaction displayed the aspect of the first-order kinetics with respect to the phenol degradation. The first-order rate equation is described as

$$\ln(C_o/C) = kt + A$$

where C is the concentration of phenol at time t (min) and C_o is the initial concentration of phenol. The k and A denote the reaction rate constant and the constant. They are evaluated from the slope and intercept of ln (C_o/C) versus t plot. The corresponding plot displays clearly a linear correlation for phenol degradation having first-order rate constant being 2.86×10^{-2} min^{-1} with respect to Ag-TiO_2 core–shell nanoparticles. The calculated phenol photodegradation rate constant for the case of TiO_2-Ag core–shell nanoparticles and TiO_2 nanoparticles were 0.89×10^{-2} and 1.68×10^{-2} min^{-1}, respectively.

The Ag-TiO_2 core–shell nanoparticles are more efficient as a photocatalyst than the TiO_2-Ag core–shell nanoparticles and TiO_2 nanoparticles. The surface plasmon of Ag works on, when the metallic core contacts with the *n*-type TiO_2 semiconductor shell, which forms a Schottky barrier band and promotes the charge separation. This phenomenon causes the formation of holes on TiO_2 valence band. These photo-generated holes at the valence band migrate to the surface and the combination with OH groups adsorbed on TiO_2 surface results in the formation of OH radicals. The electrons in conduction band combine with O_2 and forms O_2^- radical. Both these radicals oxidize phenol molecules, resulting in the formation of intermediate organic species and subsequently complete oxidation of these species to water and carbon dioxide.[32,33] The existing β-CD promotes the close contact of the TiO_2 surface with an organic molecule by a host–guest inclusion and increases the reaction rate. The possible mechanism was shown in Figure 5. In TiO_2 nanoparticles there

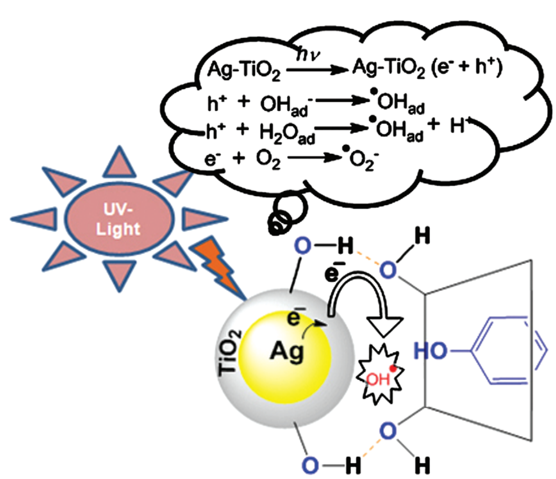

Fig. 5. Photocatalytic mechanism of β-CD-modified Ag-TiO_2 core–shell nanoparticle under UV light source.

is no such charge separation carried out between metal and metal-oxide layer and photocatalytic reaction rate is not enhanced. It should be assumed for the TiO_2-Ag core–shell nanoparticles that the outer Ag layer becomes barrier on the contact of TiO_2 surface and water molecules and hinders the formation of hydroxyl radicals, resulting in the slower rate of the photocatalysis than the case of the TiO_2-Ag core–shell nanoparticles, although the rate is higher than the case in the absence of nanoparticles.

4. CONCLUSION

The β-CD-modified highly water-dispersible Ag-TiO_2 and TiO_2-Ag core–shell nanoparticles have been successfully synthesized by an approach of green chemistry using mild conditions at room temperature. The TEM images clearly show the core and shell formation for the Ag-TiO_2 and TiO_2-Ag nanoparticles, which are uniformly spherical. It is suggested that the β-CD plays a significant role to stabilize the growing nanoparticles and disperse them well in water. The present report indicates that Ag-TiO_2 core–shell nanoparticles display a red shift of surface plasmon band which enhances photocatalytic activity. The photocatalytic degradation of phenol is faster in an aqueous suspension of β-CD modified Ag-TiO_2 core–shell nanoparticles than the β-CD modified TiO_2 nanoparticles and β-CD modified TiO_2-Ag core–shell nanoparticles. It can be concluded that the catalytic activity of TiO_2 nanoparticles is encouraged by the surface plasmon characteristics of Ag core and the host–guest inclusion characteristics of β-CD on TiO_2 shell. Then this β-CD modified core–shell photocatalyst should be the promising nanomaterials in green chemistry.

Acknowledgment: The authors are grateful to Professor Po–Da Hong, Polymer Engineering Department, National Taiwan University of Science and Technology for the measurements of UV-Vis absorption spectra.

References and Notes

1. P. V. Kamat, *J. Phys. Chem. B* 106, 7729 (**2002**).
2. T. Hirakawa and P. V. Kamat, *Langmuir* 20, 5647 (**2004**).
3. K. Matsubara and T. Tatsuma, *Adv. Mater.* 19, 2802 (**2007**).
4. J. Zeng, Q. Zhang, J. Chen, and Y. Xia, *Nano Lett.* 10, 30 (**2010**).
5. H. Sakai, D. Kanda, H. Shibata, T. Ohkubo, and M. Abe, *J. Am. Chem. Soc.* 128, 4944 (**2006**).
6. W. Wang, J. Zhang, F. Chen, D. He, and M. Anpo, *J. Colloid Interface Sci.* 323, 182 (**2008**).
7. T. Hirakawa and P. V. Kamat, *J. Am. Chem. Soc.* 127, 3928 (**2005**).
8. D. Zhang, X. Song, R. Zhang, M. Zhang, and F. Liu, *Eur. J. Inorg. Chem.* 24, 1643 (**2005**).
9. R. T. Tom, J. S. Nair, N. Singh, M. Aslam, C. L. Nagendra, R. Philip, K. Vijayamohanan, and T. Pradeep, *Langmuir* 19, 3439 (**2003**).
10. J. Sun, J. Zhuang, S. Guan, and W. Yang, *J. Nanopart. Res.* 10, 653 (**2008**).
11. Y. Nakanishi and T. Imae, *J. Colloid Interface Sci.* 285, 158 (**2005**).
12. Y. Zhou and M. Antonietti, *J. Am. Chem. Soc.* 125, 14960 (**2003**).
13. T. Ung, L. M. Liz-Marzan, and P. Mulvaney, *J. Phys. Chem. B* 103, 6770 (**1999**).
14. Y. Sun and Y. Xia, *Adv. Mater.* 14, 833 (**2002**).
15. P. D. Cozzoli, R. Comparelli, E. Fanizza, M. L. Curri, A. Agostiano, and D. Laub, *J. Am. Chem. Soc.* 126, 3868 (**2004**).
16. N. Kakuta, K. H. Park, M. F. Finlayson, A. Veno, A. J. Bard, A. Campion, M. A. Fox, S. E. Webber, and J. M. White, *J. Phys. Chem.* 89, 3828 (**1985**).
17. C. Nasr, H. S. Chandini, W. Y. Kim, R. H. Schmehl, and P. V. Kamat, *J. Phys. Chem. B* 101, 7480 (**1997**).
18. I. Pastoriza-antos, D. S. Koktysh, A. A. Mamedov, M. Giersig, N. A. Kotov, and L. M. Liz-Marzan, *Langmuir* 16, 2731 (**2000**).
19. Y. H. Kim, Y. S. Kang, and B. G. Jo, *J. Ind. Eng. Chem.* 10, 739 (**2004**).
20. T. Hirakawa and P. V. Kamat, *J. Am. Chem. Soc.* 127, 3928 (**2005**).
21. Du, J. Zhang, J. Liu, Z. Han, B. Jiang, and T. Huang, Y., *Langmuir* 22, 1307 (**2006**).
22. S. Vaidya, A. Patra, and A. K. Ganguli, *J. Nanopart. Res.* 12, 1033 (**2010**).
23. J. Szejtli and T. Osa, Comprehensive Supramolecular Chemistry, Pergamon, Oxford (**1996**). Vol. 3.
24. S. Kundu and N. Chattopadhyay, *J. Photochem. Photobiol. A* 88, 105 (**1995**).
25. N. M. Dimitrijevic, Z. V. Saponjic, D. M. Bartels, M. C. Thurnauer, D. M. Tiede, and T. Rajh, *J. Phys. Chem. B* 107, 7368 (**2003**).
26. Y. Liu, K. B. Male, P. Bouvrette, and J. H. T. Luong, *Chem. Mater.* 15, 4172 (**2003**).
27. D. Bonacchi, A. Caneschi, D. Gatteschi, C. Sangregorio, R. Sessoli, and A. Falqui, *J. Phys. Chem. Solids* 65, 719 (**2004**).
28. B. He, J. J. Tan, K. Y. Liew, and H. Liu, *J. Mol. Catal. A* 221, 121 (**2004**).
29. S. Pande, S. K. Ghosh, S. Praharaj, S. Panigrahi, S. Basu, S. Jana, A. Pal, T. Tsukuda, and T. Pal, *J. Phys. Chem. C.* 111, 10806 (**2007**).
30. G. Norwitz, J. Farino, and P. N. Keliher, *Anal. Chem.* 51, 1632 (**1979**).
31. Y. Nakanishi and T. Imae, *J. Colloid Interface Sci.* 297, 122 (**2006**).
32. R. S. Sonawane and M. K. Dongare, *J. Mol. Cataly. A: Chem.* 243, 68 (**2006**).
33. N. A. Laoufi, D. Tassalit, and F. Bentahar, *Global NEST Journal* 10, 404 (**2008**).

Received: 23 June 2010. Accepted: 26 July 2010.